AJNR

High-Resolution MRI for Evaluation of the Possibility of Successful Recanalization in Symptomatic Chronic ICA Occlusion: A Retrospective Study

M. Tang, X. Yan, J. Gao, L. Li, X. Zhe, Xin Zhang, F. Jiang, J. Hu, N. Ma, K. Ai and Xiaoling Zhang

AJNR Am J Neuroradiol published online 21 July 2022
http://www.ajnr.org/content/early/2022/07/21/ajnr.A7576

Published July 21, 2022 as 10.3174/ajnr.A7576

High-Resolution MRI for Evaluation of the Possibility of Successful Recanalization in Symptomatic Chronic ICA Occlusion: A Retrospective Study

M. Tang, X. Yan, J. Gao, L. Li, X. Zhe, Xin Zhang, F. Jiang, J. Hu, N. Ma, K. Ai, and Xiaoling Zhang

ABSTRACT

BACKGROUND AND PURPOSE: Accurate radiologic evaluation of the possibility of successful recanalization in symptomatic chronic ICA occlusion remains challenging. This study aimed to investigate the high-resolution MR imaging characteristics of symptomatic chronic ICA occlusion and their association with successful recanalization.

MATERIALS AND METHODS: Consecutive patients with symptomatic chronic ICA occlusion who underwent balloon dilation plus stent implantation were identified retrospectively and divided into 2 groups: a successful recanalization group and an unsuccessful recanalization group. Clinical and high-resolution MR imaging characteristics were compared between the groups. Univariate and multivariate analyses were used to identify the characteristics associated with successful recanalization.

RESULTS: A total of 114 patients were included in the study. High-resolution MR imaging characteristics independently associated with unsuccessful recanalization were longer lesion length (OR, 0.41; 95% CI, 0.36–0.55; $P = .009$) and larger calcification volume (OR, 0.56; 95% CI, 0.37–0.68; $P = .002$) for proximal occlusion and reversed distal ICA flow at the level of ophthalmic segment or above (OR, 0.14; 95% CI, 0.08–0.48; $P = .001$). Reversed distal ICA flow at the level of the petrous segment or below (OR, 4.07; 95% CI, 1.65–8.38; $P = .001$) and lumen area (OR, 1.13; 95% CI, 1.04–1.61; $P = .002$) for distal occlusion were risk factors of successful recanalization.

CONCLUSIONS: In symptomatic chronic ICA occlusion, lesion length and calcification volume (for proximal occlusion), the level of reversed distal ICA flow, and the lumen area (for distal occlusion) appear to be predictors of successful recanalization. High-resolution MR imaging can evaluate chronic ICA occlusion and help in clinical decision-making.

ABBREVIATIONS: CE = contrast-enhanced; CICAO = chronic ICA occlusion; HR = high-resolution; IPH = intraplaque hemorrhage; NSA = number of signals averaged

ICA occlusion occurs in 6 per 100,000 persons per year and is one of the main causes of ischemic stroke.[1,2] While recurrence is uncommon in asymptomatic patients, 10%–18% of symptomatic patients will experience another cerebral ischemic event within 1 year. In chronic ICA occlusion (CICAO), morbidity and mortality are 40%–69%, and 16%–55%, respectively.[3,4] Studies have demonstrated decreased psychomotor speed, executive function, and working memory in patients with CICAO,[5,6] and a possible relationship between CICAO and cognitive impairment has been suggested.

Recanalization of CICAO can restore blood supply to ischemic brain tissue, reduce mortality and disability rates, and improve neurocognitive function[7-9] and quality of life. Successful recanalization is achieved in 23%–93% of patients.[10-13] The possibility of success depends on factors such as the duration of the occlusion,[14] the length of the occlusion, the composition of the thrombus or plaque,[15-17] the stump condition[18,19] of occluded vessels, and the adequacy of collateral circulation.[20]

In CICAO, the real duration of occlusion is not known, so indirect estimations are made on the basis of the time of onset of symptoms and the imaging features. DSA, CTA, ultrasound, and MR imaging are complementary modalities for the evaluation of CICAO. DSA can dynamically display the stump condition, occlusion length, distal reflux, and collateral circulation, but it cannot analyze the course or the wall and lumen of occluded vessels.[21-23] CTA can reliably demonstrate occlusion length, collateral circulation, and the course of occluded vessels, but it cannot accurately analyze the

Received January 13, 2022; accepted after revision May 31.

From the Departments of MRI (M.T., X.Y., J.G., L.L., X. Zhe., X. Zhang., N.M., X. Zhang) and Neurology (F.J., J.H.), Shaanxi Provincial People's Hospital, Beilin District, Xi'an City, Shaanxi Province, China; and Department of Clinical Science (K.A.), Philips Healthcare, Xian, China.

This research was supported by the Shanxi Provincial Key Research and Development Project of Shaanxi Province of China (2021SF-064).

Please address correspondence to Xiaoling Zhang, MD, Department of MRI, Shaanxi Provincial People's Hospital, Beilin District, Xi'an City 710068, Shaanxi Province, China; e-mail: zxl.822@163.com

http://dx.doi.org/10.3174/ajnr.A7576

age of the thrombus, the components of plaque, or the intracranial ICA (because of intervening skull bone).[19,24] Ultrasound is a noninvasive, economical, and highly operator-dependent tool for the evaluation of carotid artery occlusion; it can show the plaque composition but is useful only for analysis of the extracranial ICA.[25] High-resolution MR imaging (HR-MR imaging), which is being increasingly used in the evaluation of intracranial and extracranial vascular diseases, can provide direct visualization of the vessel wall and lumen, composition of the thrombus or plaque, occlusion length, collateral circulation, and the course of the occluded vessels[26-28] and can compensate for the weaknesses of other imaging modalities.

We hypothesized that accurate evaluation of symptomatic CICAO using HR-MR imaging may help in the choice of treatment strategy, improve the success rate of interventional treatment, and reduce perioperative complications. The purpose of this retrospective study was to identify the HR-MR imaging characteristics of symptomatic patients with CICAO who were successfully recanalized. This information will be of use to clinicians during treatment selection and help avoid complications.

MATERIALS AND METHODS

Patients

We retrospectively analyzed consecutive CICAO recanalizations attempted at Shaanxi Provincial People's Hospital between October 2014 and December 2021. All patients underwent HR-MR imaging before the procedure. Patients were eligible for inclusion if they had the following:[29] 1) ipsilateral transient cerebral ischemia, ischemic stroke, or amaurosis for >1 month; 2) unilateral ICA occlusion diagnosed by CTA, ultrasound, or contrast-enhanced (CE)-MRA; 3) the diagnosis of CICAO confirmed by DSA; and 4) failure of medical treatment. Exclusion criteria included dissection, cardiogenic embolism, allergy to contrast medium, bleeding tendency, and poor-quality imaging. Clinical data, which included the patient's age, smoking, hypertension, diabetes mellitus, hyperlipidemia, history of stroke and stroke, and imaging data, were collected from the hospital records for analysis.

This study was approved by the Ethics Committee of Shaanxi Provincial People's Hospital (Xian, Shaanxi Province, China). Informed consent form was signed by all participants.

HR-MR Imaging

HR-MR imaging was performed with the patient in a supine position. A 16-channel head-neck coil was used with an Ingenia 3T MR imaging scanner (Philips Healthcare). The HR-MR imaging protocol included TOF-MRA, 3D-T1WI, T1WI-TSE and T2WI-TSE, CE-MRA, and CE 3D-T1WI. The axial views were perpendicular to the arterial course. Scan parameters for the different sequences were as follows: 3D-T1WI and CE 3D-T1WI: FOV = 200 × 200 mm^2, TR/TE = 1000/16 ms, acquisition matrix = 400 × 400, image resolution = 0.5 × 0.5 × 0.5 mm^3, number of signals averaged (NSA) = 1, acceleration factor = 2; CE-MRA: FOV = 320 × 320 mm^2, TR/TE = 175/4.8 ms, acquisition matrix = 456 × 456, image resolution = 0.7 × 0.7 mm^3, dynamic scans = 3, NSA = 1; T1WI-TSE: FOV = 140 × 101 mm^2, TR/TE = 477/13 ms, acquisition matrix = 312 × 216, image resolution = 0.45 × 0.45 mm^3, NSA = 2; T2WI-TSE: FOV = 140 × 101 mm^2, TR/TE = 3000/90 ms, acquisition matrix = 312 × 216, image resolution = 0.45 × 0.45 mm^3, NSA = 2. CE T1WI was performed following intravenous administration of gadoterate meglumine at a dose of 0.1 mmol/kg. The total acquisition time was approximately 30 minutes.

Image Analysis

The image quality was divided into 4 levels:[30] Poor indicated that the outline of vessel wall and lumen was unclear accompanied by obvious artifacts; medium, the parts of the wall and lumen were clear with a few artifacts; good, the wall and lumen were clear with a few artifacts; excellent, the wall and lumen were clear without artifacts. Image quality below medium could not be analyzed. Raw data were imported into Plaque View postprocessing software (VPDiagnostics) to generate axial, coronal, and sagittal reconstructions of the CICAO. The senior neuroradiologists (X. Zhe and X. Yan, each with 5 years' experience in interpreting HR-MR imaging of the arterial wall), who were blinded to the patients' clinical information, independently analyzed the images for plaque composition, shape of the stump, and signal characteristics of the wall and lumen in proximal and distal ICA occlusions, location of contrast agent reflux, and the collateral circulation. Differences in interpretation were settled by discussion. Imaging characteristics at the proximal and distal occlusive segments (ie, collateral circulation, location of contrast agent reflux, morphologic characteristics of the stump, and the lumen and wall of the occluded segment) were noted.

We first used CE-MRA to assist in localization and then find collateral circulation vessels and to evaluate collateral vessel diameter on HR-MRI. Collateral circulation was divided into primary (anterior or posterior communicating artery) and secondary (ophthalmic artery and meningeal artery) collaterals.[31] Primary collateral vessels were graded as follows: 1, absent; 2, probably present; 3, definitely present or greater than the normal side. Adequate primary collateral vessels were defined as grade 3. Secondary collateral vessels were graded in the comparison of the symptomatic and normal side as follows: 1, absent; 2, less than the normal side; 3, equal to the normal side; 4, greater than the normal side. "Diminished" was defined as grades 1–2, and "adequate" was defined as grades 3–4.[32] "Distal reflux" was defined as the presence of contrast agent in the ICA distal to the occlusion on CE-MRA and the lumen showing no signal on HR-MRI during the ipsilateral injection; the location of reflux was categorized as the petrous segment or below, cavernous segment, clinoid segment, ophthalmic segment, or communicating segment.[18] The stump, if present, was categorized as tapered and nontapered if there was contrast filling within the segment of the cervical ICA after it bifurcates from the common carotid artery proximal to the occluded segment. Hyperintensity, isointensity, and hypointensity were defined as higher, equal, and lower intensity, respectively, relative to the sternocleidomastoid muscle at the same level.[33]

Lipid-rich necrotic core, calcification, hemorrhage, loose matrix, and dense fibrous tissue were identified using MR imaging criteria.[34] The proximal occlusion segment—extending from the occlusion site to the site of disappearance of signal or the appearance of significantly different signal in the lumen—was the primary lesion. Its length and plaque composition were measured (Fig 1*A–C* and Fig 2*B*). Distal occlusion was defined as the secondary lesion, with no enhancement in the lumen. Three measurement

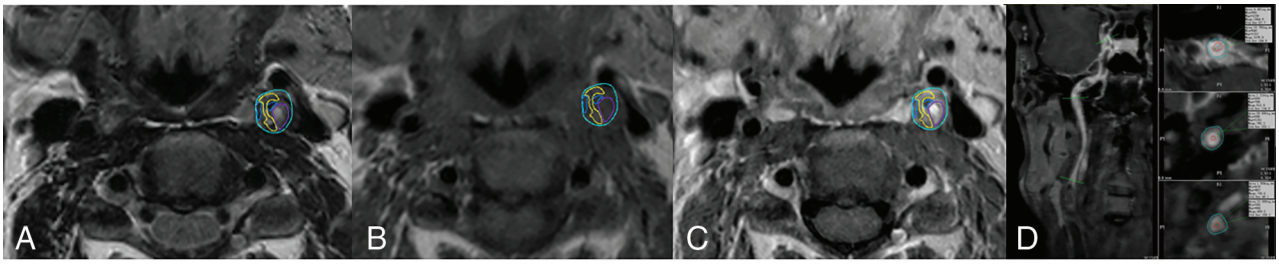

FIG 1. *A–C*, T2WI, T1WI, and CE-T1WI show the measurement of the proximal segment; the loose matrix (purple) shows hyperintensity on T2WI, iso- or hypointensity on T1WI, and enhancement on CE-T1WI. Calcification (blue) appears as hypointensity on all sequences; hemorrhage (orange) appears as hyperintensity on T1WI, iso- or hypointensity on T2WI, and no enhancement on CE-T1WI. The lipid-rich necrotic core (yellow) shows iso- or hyperintensity on T1WI, iso- or hyperintensity on T2WI, and enhancement on CE-T1WI. *D*, The lumen and wall area were measured in the distal occlusion.

points were selected in the distal occlusion segment (proximal, middle, and distal; Fig 1*D*). Then, the average lumen and wall values of the 3 points were obtained. An independent interventionist reviewed the procedural angiograms off-line and recorded the morphologic characteristics of the stump and occlusion segment.

Interventional Therapy

Antiplatelet therapy (aspirin, 100 mg, and clopidogrel, 75 mg daily) was started before the operation. Heparin was administered to maintain an activated clotting time within the range of 200–250 seconds. An 8F femoral sheath was inserted into the common carotid artery, and a guidewire and a multifunctional angiography catheter were inserted through it using the Seldinger technique. Angiography was performed to define the position of the ICA occlusion and observe the stump, distal ICA, reflux position, and collateral circulation. A microwire was passed through the occluded ICA segment. When the wire had entered the distal true lumen, it was exchanged for a 1.5-mm-diameter coronary balloon for predilation. A distal embolic protection device (SpiderFX, 4 mm; Medtronic) was deployed if an adequate landing zone was identified. The occluded segment of the ICA was dilated by the balloon, and a self-expandable stent of the appropriate size was placed.

Outcome of Events

Success was defined as[18] successful stent placement of the occlusion segment, with a final residual stenosis of ≤20% and establishment of grade III TICI antegrade flow, without the patient experiencing any complications. The procedure was deemed unsuccessful under the following circumstances: 1) The patient experienced complications after stent placement, or 2) no retrograde blood flow was observed after recanalization. Complications included ICA dissection, appearance of cerebral infarction in >1 lobe, cerebral hemorrhage, ipsilateral retinal infarction, reocclusion in the perioperational stage, and death. Finally, the patients were divided into 2 groups: a successful group, comprising patients who underwent successful recanalization without experiencing any complication, and an unsuccessful group, comprising patients who had recanalization failure and/or experienced complications.

Statistical Analysis

The normality test of continuous variable distribution was performed first. Then the variables were presented as mean (SD) or median (interquartile range) accordingly. The Student *t* test or the Mann-Whitney *U* test was used to compare differences in means or interquartile ranges between groups, and the χ^2 test or the Fisher exact test was used to compare differences in proportions, respectively. The intraclass correlation coefficient was used to assess interobserver consistency in the interpretation of HR-MR imaging. κ analysis was used to assess agreement between HR-MR imaging and DSA and was graded as good ($\kappa \geq 0.75$), moderate ($0.75 > \kappa \geq 0.4$), or poor ($\kappa < 0.4$). Multivariable logistic regression was applied to identify the independent predictors of recanalization failure, and a forward likelihood ratio method with a significance level for entry of .05 was performed to select variables included in the model. Statistical analysis was performed using SPSS 22.0 (IBM.). $P \leq .05$ indicated a statistically significant difference.

RESULTS

Clinical Data

From among the 129 patients who met the inclusion criteria, we excluded 15 patients; these included patients with CICAO related to trauma ($n = 2$), arteritis ($n = 4$), and Moyamoya disease ($n = 3$), as well as those with poor-quality imaging ($n = 6$). The 114 patients included in this study had a median age of 57 years (interquartile range, 32–73 years). Presentations were with transient cerebral ischemia, retinal ischemia, or stroke. Recanalization was successful in 76/114 (66.7%) patients (the successful group), but it was unsuccessful in 38/114 (33.3%) patients (the unsuccessful group). While recanalization failed in 34/114 (29.8%) patients, 4/114 (3.5%) patients had complications after recanalization; the complications included ICA dissection ($n = 1$), intracranial hemorrhage ($n = 2$), and cerebral infarction progression ($n = 1$). Table 1 summarizes the characteristics of the patients.

HR-MR Imaging Features

A tapered stump was observed in 64/114 (56.1%) patients and in 48/76 (63.2%) patients in the successful group (Fig 2*C*, *-D*). Secondary collateral circulation was more often seen in the unsuccessful group (Fig 3*C*, *-E*) than in the successful group ($P = .025$). Among the 114 patients, the level of reversed distal ICA flow was visualized at the communicating segment, ophthalmic segment, clinoid segment, cavernous segment, and petrous segment or below in 7%, 10.5%, 20.2%, 28.1%, and 34.2% patients, respectively. The reversed distal ICA flow tended to be at lower levels in the successful group than in the unsuccessful group ($P < .001$; Fig 2*A–C*; Fig 3*A*,

Table 1: Characteristics of patients with CICAO

	Successful (n = 76)	Unsuccessful (n = 38)	P
Age (mean) (yr)	53.9 (SD, 15.9)	58.5 (SD, 11.0)	.115
Male (No.) (%)	49 (64.5)	23 (60.5)	.680
Smoking (No.) (%)	44 (57.9)	26 (68.4)	.276
Hypertension (No.) (%)	29 (38.1)	14 (36.8)	.891
Diabetes mellitus (No.) (%)	22 (28.9)	5 (13.2)	.062
Hyperlipidemia (No.) (%)	39 (51.3)	15 (39.5)	.233
History of stroke (No.) (%)	12 (15.8)	8 (21.1)	.500
Stroke (No.) (%)	55 (72.4)	32 (84.2)	.161

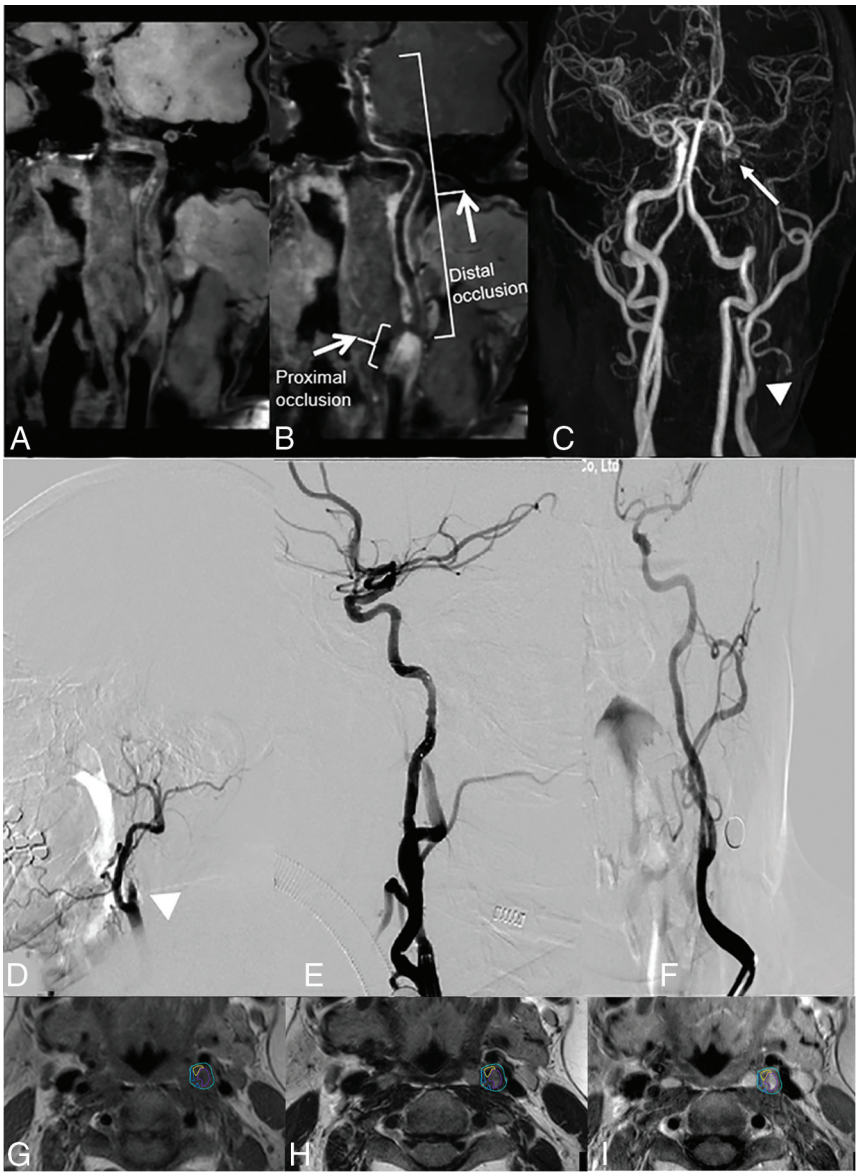

FIG 2. Successful recanalization cases. *A*, Curved planar reformation (CPR) on T1WI-volume isotropic turbo spin-echo acquisition (VISTA) shows moderate hypointensity in the proximal occlusion and iso- or hypointensity in the lumen of the distal occlusion. *B*, CPR on T1WI-VISTA-CE shows inhomogeneous enhancement in the origin of the left ICA and hypointensity in the distal occlusion. *C* and *D*, CE-MRA and preoperative DSA show a tapered stump (*triangle*) and reversal of flow above the clinoid segment of left ICA (*arrow*). *E* and *F*, Postoperative DSA shows successful recanalization. *G–I*, Plaque composition is shown in the proximal occlusion on T1WI and T2WI and enhancement on T1WI (blue, calcification; orange, hemorrhage; yellow, lipid-rich/necrotic core; purple, loose matrix).

B, C, E). The mean volume of lipid-rich necrotic core (for proximal occlusion, Fig 2*G–I*; Fig 3*F–H*) and lumen iso- or hypointensity and lumen area (for distal occlusion, Figs 2 and 3 *A*, *-B*) were significantly larger in the successful group than in the unsuccessful group (167.2 [SD, 74.2] mm^3 versus 139.8 [SD, 54.5] mm^3, $P < .050$; 59.2% versus 39.5%, $P = .047$; 7.4 [SD, 3.4] mm^2 versus 3.9 [SD, 2.3] mm^2, $P < .001$, respectively). The mean lesion length and calcification volume (for proximal occlusion, Fig 2*A, B, G–I*; Fig 3*A, B, F–H*) were significantly lower in the successful group than in the unsuccessful group (20.7 [SD, 5.4] mm versus 23.9 [SD, 4.8] mm, $P < .005$, and 41.3 [SD, 39.5] mm^3 versus 141.9 [SD, 107.8] mm^3, $P < .001$, respectively). Lesion volume, hemorrhage, dense fibrous tissue, loose matrix (for proximal occlusion); wall area (for distal occlusion); and primary collateral circulation were not significantly different between the 2 groups ($P > .05$). Table 2 summarizes the lesion characteristics.

Relationship between HR-MR Imaging Features and Success of Recanalization

In univariate analysis, the presence of a tapered stump, reversed distal ICA flow at the petrous segment or below, larger volume of the lipid-rich necrotic core (for proximal occlusion), and lumen iso- or hypointensity and larger lumen area (for distal occlusion) were significantly associated with successful recanalization (all, $P < .05$). Conversely, reversed distal ICA flow at the ophthalmic segment or above, longer lesion length, and more calcification volume (for proximal occlusion) were significantly associated with failure of recanalization (all, $P < .05$). In multivariate analysis, the following variables were protective factors of successful recanalization: lesion length: OR, 0.41; 95% CI, 0.36–0.55; $P = .009$; larger calcification volume for proximal occlusion: OR, 0.56; 95% CI, 0.37–0.68; $P = .002$; and reversed distal ICA flow at the ophthalmic segment or above: OR, 0.14; 95% CI, 0.08–0.48; $P = .001$; Table 3. The following variables were risk factors for successful recanalization: reversed distal ICA flow at petrous segment or below: OR, 4.07; 95% CI, 1.65–8.38; $P = .001$;

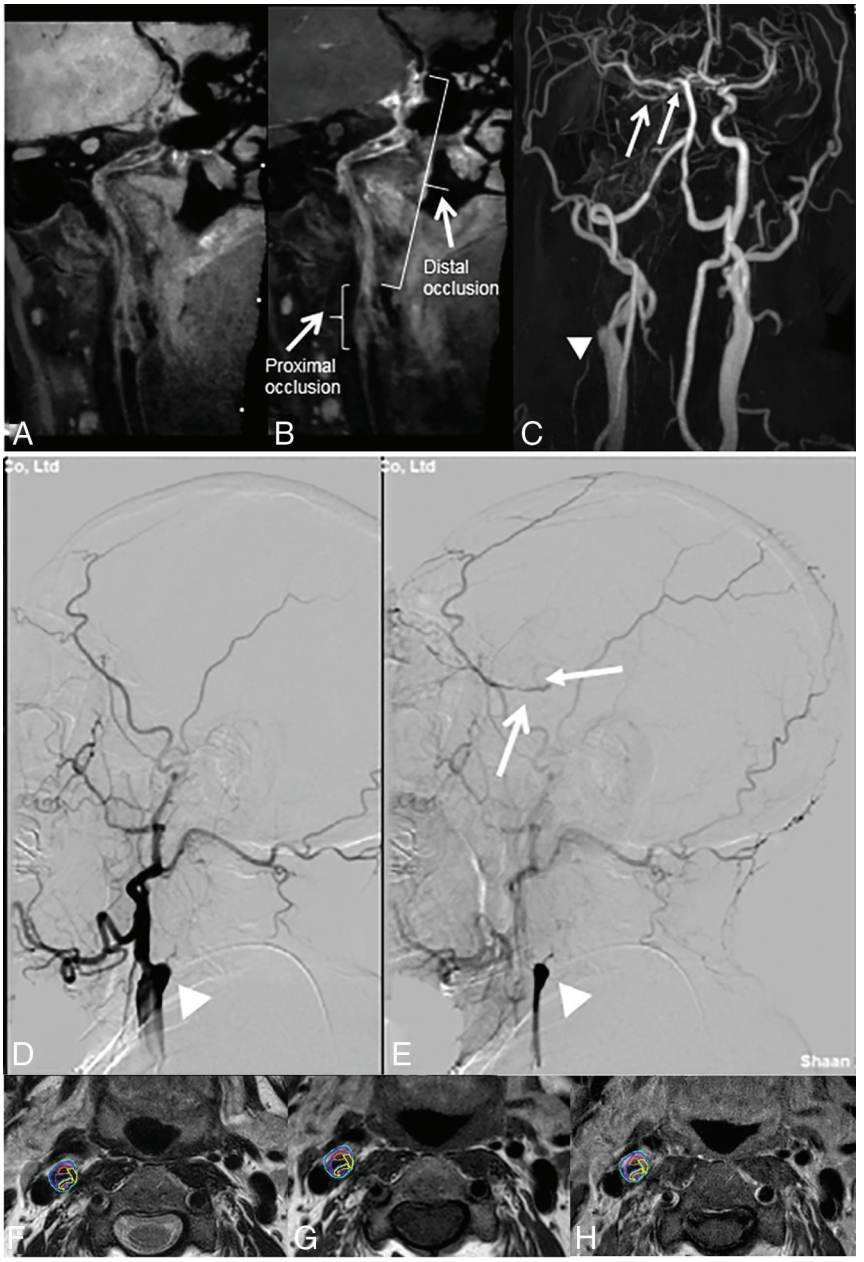

FIG 3. Unsuccessful recanalization cases. *A*, Curved planar reformation (CPR) on TIWI-volume isotropic turbo spin-echo acquisition (VISTA) shows mixed signal and wall collapse in the lumen distal to the occlusion. *B*, CPR on TIWI-VISTA-CE shows inhomogeneous enhancement in the proximal occlusion and distal segment of the right ICA (*arrowhead*). *C–E*, CE-MRA and DSA show a blunt stump (*triangle*), secondary collateral circulation (*arrowhead*), and reversal flow above the communicating segment of right ICA (*arrows*). *F–H*, Plaque composition is shown in the proximal occlusion (blue, calcification; orange, hemorrhage; yellow, lipid-rich/necrotic core; purple, loose matrix).

and larger lumen area for distal occlusion: OR, 1.13; 95% CI, 1.04–1.61; $P = .002$; Table 3.

Reproducibility Assessment between DSA and MR Imaging

There was good agreement between DSA and HR-MRI for the evaluation of stump status, the level of reversed distal ICA flow, and major and minor collateral circulations ($\kappa = 0.92$, $\kappa = 0.88$, $\kappa = 0.89$, and $\kappa = 0.84$, respectively). The intraclass correlation coefficients for lesion length, lesion volume, lipid-rich necrotic core, hemorrhage, calcification, dense fibrous tissue, loose matrix (for proximal occlusion), and lumen area and wall area (for distal occlusion) were 0.94, 0.87, 0.78, 0.76, 0.81, 0.84, 0.88, 0.91, and 0.90, respectively.

DISCUSSION

HR-MR imaging has a crucial role in the imaging evaluation of symptomatic patients with CICAO. HR-MR imaging can accurately evaluate the vessel lumen, wall, and course; it can provide information on the degree of inflammation of the wall and the collateral circulation and distinguish lumen blood stasis and thrombus distal to the occlusion.[35,36] In this study, the HR-MR imaging characteristics of patients with successful recanalization included a tapered stump, less secondary collateral circulation, reversed distal ICA flow at the level of petrous segment or below, more lipid-rich necrotic core, less calcification volume, shorter lesion length (for proximal occlusion), and lumen iso- or hypointensity and larger lumen area (for distal occlusion). Multivariate analysis showed that shorter lesion length and less calcification volume (for proximal occlusion) and reversed distal ICA flow at the petrous segment or below and larger lumen area (for distal occlusion) were independent predictors of successful recanalization.

Atherosclerosis is responsible for 70% of cases of CICAO. Because patients are asymptomatic in the early stages, the real duration of occlusion cannot be accurately defined.[37] With prolongation of the occlusion time, the stump morphology changes from tapered to blunt or no stump, the proximal plaque and distal lumen thrombus hardens due to fibrosis and calcification, and the occlusive length gradually increases due to the thrombotic process and a collapsed lumen in the distal occlusion.[38] These changes increase the difficulty of recanalization in CICAO, as has also been observed in chronic coronary occlusion.[14]

Our study showed that reversed distal ICA flow at the petrous segment or below was a risk factor for successful recanalization in CICAO, while reversed distal flow at the ophthalmic segment or above was a protective factor of success. This finding is consistent with those in previous studies.[11,18] In addition, we found that successful recanalization was also related to lesion length and calcification volume (for proximal occlusion) and lumen area (for distal occlusion). A previous study showed that HR-MR imaging can

Table 2: HR-MR imaging characteristics of lesions in symptomatic patients with CICAO

	Total (n = 114)	Successful (n = 76)	Unsuccessful (n = 38)	P
Right (No.) (%)	67 (58.8)	42 (55.2)	25 (65.8)	.282
Tapered stump (No.) (%)	64 (56.1)	48 (63.2)	16 (42.1)	.033
Level of reversed distal ICA flow				<.001
Communicating segment (No.) (%)	8 (7.0)	2 (2.6)	6 (15.8)	
Ophthalmic segment (No.) (%)	12 (10.5)	2 (2.6)	10 (26.3)	
Clinoid segment (No.) (%)	23 (20.2)	14 (18.4)	9 (23.7)	
Cavernous segment (No.) (%)	32 (28.1)	24 (31.6)	8 (21.1)	
Petrous segment or below (No.) (%)	39 (34.2)	34 (44.7)	5 (13.2)	
Collateral circulation				
Primary (No.) (%)	64 (56.1)	39 (51.3)	25 (65.8)	.142
Secondary (No.) (%)	25 (21.9)	12 (15.7)	13 (34.2)	.025
Proximal occlusion				
Lesion length (mean) (mm)	21.9 (SD, 4.2)	20.7 (SD, 5.4)	23.9 (SD, 4.8)	<.005
Lesion volume (mean) (mm^3)	1084.8 (SD, 472.5)	1007.3 (SD, 453.4)	1159.1 (SD, 486.1)	.110
Lipid-rich necrotic core (mean) (mm^3)	143.3 (SD, 76.6)	167.2 (SD, 74.2)	139.8 (SD, 54.5)	<.050
Hemorrhage (mean) (mm^3	54.5 (SD, 43.1)	58.4 (SD, 46.7)	53.6 (SD, 40.4)	.510
Calcification (mean) (mm^3)	112.9 (SD, 96.4)	41.3 (SD, 39.5)	141.9 (SD, 107.8)	<.001
Dense fibrous tissue (mean) (mm^3)	708.2 (SD, 391.1)	689.6 (SD, 372.3)	738.8 (SD, 437.6)	.611
Loose matrix (mean) (mm^3)	250.3 (SD, 130.5)	219.7 (SD, 103.8)	257.9 (SD, 141.6)	.120
Distal occlusion				
Lumen iso -to hypointensity (No.) (%)	60 (52.6)	45 (59.2)	15 (39.5)	.047
Lumen area (mean) (mm^2)	6.28 (SD, 3.5)	7.4 (SD, 3.4)	3.9 (SD, 2.3)	<.001
Wall area (mean) (mm^2)	32.7 (SD, 6.9)	32.0 (SD, 6.8)	33.4 (SD, 8.7)	.340

Table 3: Factors associated with recanalization success in univariable and multivariable analysis

	Univariable Analysis		Multivariable Analysis	
Characteristic	OR (95% CI)	P	OR (95% CI)	P
Right	0.64 (0.51–1.33)	.282		
Tapered stump	2.36 (1.02–3.11)	.035	2.23 (0.87–3.36)	.091
Level of reversed distal ICA flow				
Communicating segment	0.14 (0.07–0.21)	.001	0.13 (0.07–0.24)	.010
Ophthalmic segment	0.08 (0.03–0.44)	<.001	0.14 (0.08–0.48)	.001
Clinoid segment	0.73 (0.63–1.21)	.214	0.62 (0.36–1.22)	.160
Cavernous segment	1.73 (0.96–3.89)	.07	1.66 (0.87–3.54)	.550
Petrous segment or below	5.34 (1.41–11.37)	<.001	4.07 (1.65–8.38)	.001
Collateral circulation				
Primary	0.55 (0.35–1.59)	.143		
Secondary	0.36 (0.14–0.71)	.027	1.32 (0.98–1.47)	.210
Proximal occlusion				
Lesion length	0.51 (0.13–0.74)	.005	0.41 (0.36–0.55)	.009
Lesion volume	2.11 (0.71–4.49)	.110		
Lipid-rich necrotic core	3.26 (1.45–6.36)	.024	2.36 (0.94–5.33)	.060
Hemorrhage	1.35 (0.65–2.38)	.510		
Calcification	0.71 (0.44–0.90)	<.001	0.56 (0.37–0.68)	.002
Dense fibrous tissue	3.31 (0.93–10.36)	.615		
Loose matrix	1.66 (0.87–3.88)	.120		
Distal occlusion				
Lumen iso- to hypointensity	2.23 (1.06–5.29)	.047	1.87 (0.91–4.66)	.091
Lumen area	1.32 (1.02–2.17)	<.001	1.13 (1.04–1.61)	.002
Wall area	1.76 (0.71–3.38)	.230		

accurately indicate the hardness of plaque by identifying its composition.[39] Chronic atherosclerotic plaque is hard (fibrotic-calcified plaque) due to the presence of relatively more calcification and dense fibrous tissue and less lipid-necrotic core.[39,40] Hard plaque and longer occlusion length at the proximal occlusion can make wiring across the occlusion difficult and result in vessel injury and arterial dissection. With prolongation of the occlusion time, the lumen distal to the occlusion wall collapses. In this study, we found that the lumen area for distal occlusion was a risk factor of successful recanalization. The lumen area was higher in the successful recanalization group than in the failed group, in which the lumen area for distal occlusion reflected the degree of collapsed vessel wall and affected the successful recanalization. HR-MR imaging can display these features, which are important reasons for failure of recanalization of CICAO. Archie,[41] therefore, suggested that when the distal ICA occlusion is small or poorly visualized, carotid endarterectomy should be performed.

In this study, tapered stump, lipid-rich necrotic core (for proximal occlusion), and lumen iso- or hypointensity (for distal occlusion) were more prevalent in the successful group. However, in

multivariable analysis, these factors were not independently associated with successful recanalization and may not be the main factors related to it. For distal occlusion, the size and composition of the thrombus may affect the success of recanalization.[42] The histologic characteristics of the thrombus might reflect the pathologic process of CICAO.[43,44] MR imaging can accurately define the duration of thrombosis in vivo through signal changes.[45] However, in some of our patients, lumen iso- or hypointensity for the distal occlusions was recanalized after stent implantation and no thrombi were found in the distal embolic protection device. We speculate that, for distal occlusion, lumen iso- or hypointensity might indicate blood stagnation.

DSA remains the criterion standard for the diagnosis of CICAO because it can accurately evaluate the stump, the position of reflux, and the collateral blood supply beyond the occlusion that flows retrograde into the distal ICA. We found good consistency between HR-MR imaging and DSA in the evaluation of stump status, the level of reversed distal ICA flow, and primary and secondary collateral circulation. The limitation of HR-MR imaging is that it cannot evaluate direction of flow. Meanwhile, DSA cannot analyze the course or wall and lumen of the occluded segment of the vessel;[22,23] moreover, it is an expensive, invasive procedure involving exposure to radiation. Although the key predictors of successful recanalization can be obtained using CTA, it cannot be used to accurately assess the intracranial ICA for intervening skull bone, the age of thrombus, intraplaque hemorrhage (IPH), and lipid-rich necrotic core. Currently, the IPH and lipid-rich necrotic core are possible to detect using CT and MR imaging, but the limitation of CT is that the IPH cannot be distinguished from lipid-rich necrotic core for overlapping density values.[46,47] Some authors have suggested that HR-MRI is the best imaging technique for the detection of IPH.[48] Otherwise, the view that HR-MRI can sensitively detect IPH has been strengthened by the Vessel Wall Imaging Study Group.[49] HR-MR imaging—which is a noninvasive, higher soft-tissue contrast, and radiationless evaluation of the vessel wall and lumen, plaque composition, the vessel distal to the occlusion, and the collateral blood supply beyond the occlusion—can, therefore, be expected to become a first-line technique for preoperative evaluation of CICAO.

This study has several limitations. First, this was a retrospective study, so a selection bias cannot be ruled out. Second, we did not analyze other imaging indices such as the structure and perfusion of brain parenchyma; this analysis might have affected the outcome. Third, when HR-MR imaging is used to observe collateral circulation, only the thickness of collateral vessels can be judged, not the direction of blood flow and leptomeningeal collateral circulation, possibly affecting the results.

CONCLUSIONS

HR-MR imaging is a noninvasive tool that can evaluate CICAO and guide decision-making in symptomatic patients with CICAO. Lesion length and calcification volume (for proximal occlusion), the level of reversed distal ICA flow, and lumen area (for distal occlusion) appear to be associated with the success of recanalization performed using balloon dilation and stent implantation. Further studies are needed to clarify how HR-MR imaging characteristics can be applied for selection of the treatment method.

Disclosure forms provided by the authors are available with the full text and PDF of this article at www.ajnr.org.

REFERENCES

1. Flaherty ML, Flemming KD, McClelland R, et al. **Population-based study of symptomatic internal carotid artery occlusion: incidence and long-term follow-up.** *Stroke* 2004;35:e349–52 CrossRef Medline
2. Iwata T, Mori T, Tajiri H, et al. **Long-term angiographic and clinical outcome following stenting by flow reversal technique for chronic occlusions older than 3 months of the cervical carotid or vertebral artery.** *Neurosurgery* 2012;70:82–90 CrossRef Medline
3. Powers WJ, Derdeyn CP, Fritsch SM, et al. **Benign prognosis of never-symptomatic carotid occlusion.** *Neurology* 2000;54:878–82 CrossRef Medline
4. Buslovich S, Hines GL. **Spontaneous recanalization of chronic internal carotid artery occlusions: report of 3 cases.** *Vasc Endovascular Surg* 2011;45:93–97 CrossRef Medline
5. Chmayssani M, Festa JR, Marshall RS. **Chronic ischemia and neurocognition.** *Neuroimaging Clin N Am* 2007;17:313–24 CrossRef Medline
6. Kao HL, Hung CS, Li HY, et al. **Long-term outcomes after endovascular recanalization in patients with chronic carotid artery occlusion.** *Am J Cardiol* 2018;122:1779–83 CrossRef Medline
7. Lin MS, Chiu MJ, Wu YW, et al. **Neurocognitive improvement after carotid artery stenting in patients with chronic internal carotid artery occlusion and cerebral ischemia.** *Stroke* 2011;42:2850–54 CrossRef Medline
8. Chen YH, Lin MS, Lee JK, et al. **Carotid stenting improves cognitive function in asymptomatic cerebral ischemia.** *Int J Cardiol* 2012;157:104–07 CrossRef Medline
9. Huang CC, Chen YH, Lin MS, et al. **Association of the recovery of objective abnormal cerebral perfusion with neurocognitive improvement after carotid revascularization.** *J Am Coll Cardiol* 2013;61:2503–09 CrossRef Medline
10. Rubiera M, Ribo M, Delgado-Mederos R, et al. **Tandem internal carotid artery/middle cerebral artery occlusion: an independent predictor of poor outcome after systemic thrombolysis.** *Stroke* 2006;37:2301–05 CrossRef Medline
11. Lee CW, Lin YH, Liu HM, et al. **Predicting procedure successful rate and 1-year patency after endovascular recanalization for chronic carotid artery occlusion by CT angiography.** *Int J Cardiol* 2016;221:772–76 CrossRef Medline
12. Kappelhof M, Marquering HA, Berkhemer OA, et al. **Intra-arterial treatment of patients with acute ischemic stroke and internal carotid artery occlusion: a literature review.** *J Neurointerv Surg* 2015;7:8–15 CrossRef Medline
13. Duijsens HM, Spaander F, van Dijk LC, et al. **Endovascular treatment in patients with acute ischemic stroke and apparent occlusion of the extracranial internal carotid artery on CTA.** *J Neurointerv Surg* 2015;7:709–14 CrossRef Medline
14. Morino Y, Abe M, Morimoto T, et al; J-CTO Registry Investigators. **Predicting successful guidewire crossing through chronic total occlusion of native coronary lesions within 30 minutes: the J-CTO (Multicenter CTO Registry in Japan) score as a difficulty grading and time assessment tool.** *JACC Cardiovasc Interv* 2011;4:213–21 CrossRef Medline
15. Liebeskind DS, Sanossian N, Yong WH, et al. **CT and MRI early vessel signs reflect clot composition in acute stroke.** *Stroke* 2011;42:1237–43 CrossRef Medline
16. Puig J, Pedraza S, Demchuk A, et al. **Quantification of thrombus Hounsfield units on noncontrast CT predicts stroke subtype and early recanalization after intravenous recombinant tissue plasminogen activator.** *AJNR Am J Neuroradiol* 2012;33:90–96 CrossRef Medline
17. Mo L, Ma G, Dai C, et al. **Endovascular recanalization for symptomatic subacute and chronically occluded internal carotid artery:**

feasibility, safety, a modified radiographic classification system, and clinical outcomes. *Neuroradiology* 2020;62:1323–34 CrossRef Medline
18. Chen YH, Leong WS, Lin MS, et al. **Predictors for successful endovascular intervention in chronic carotid artery total occlusion.** *JACC Cardiovasc Interv* 2016;9:1825–32 CrossRef Medline
19. Michel P, Ntaios G, Delgado MG, et al. **CT angiography helps to differentiate acute from chronic carotid occlusion: the "carotid ring sign."** *Neuroradiology* 2012;54:139–46 CrossRef Medline
20. Hugenholtz H, Elgie RG. **Carotid thromboendarterectomy: a reappraisal: criteria for patient selection.** *J Neurosurg* 1980;53:776–83 CrossRef Medline
21. Zanaty M, Howard S, Roa JA, et al. **Cognitive and cerebral hemodynamic effects of endovascular recanalization of chronically occluded cervical internal carotid artery: single-center study and review of the literature.** *J Neurosurg* 2019;132:1158–66 CrossRef Medline
22. Wang X, Wang Z, Ji Y, et al. **Enterprise stent in recanalizing non-acute atherosclerotic intracranial internal carotid artery occlusion.** *Clin Neurol Neurosurg* 2017;162:47–52 CrossRef Medline
23. Namba K, Shojima M, Nemoto S. **Wire-probing technique to revascularize subacute or chronic internal carotid artery occlusion.** *Interv Neuroradiol* 2012;18:288–96 CrossRef Medline
24. Hong JM, Lee SE, Lee SJ, et al. **Distinctive patterns on CT angiography characterize acute internal carotid artery occlusion subtypes.** *Medicine (Baltimore)* 2017;96:e5722 CrossRef Medline
25. Liu Y, Jia L, Liu B, et al. **Evaluation of endarterectomy recanalization under ultrasound guidance in symptomatic patients with carotid artery occlusion.** *PloS One* 2015;10:e0144381 CrossRef Medline
26. Jiang Y, Zhu C, Peng W, et al. **Ex-vivo imaging and plaque type classification of intracranial atherosclerotic plaque using high resolution MRI.** *Atherosclerosis* 2016;249:10–16 CrossRef Medline
27. Bodle JD, Feldmann E, Swartz RH, et al. **High-resolution magnetic resonance imaging: an emerging tool for evaluating intracranial arterial disease.** *Stroke* 2013;44:287–92 CrossRef Medline
28. Cai JM, Hatsukami TS, Ferguson MS, et al. **Classification of human carotid atherosclerotic lesions with in vivo multicontrast magnetic resonance imaging.** *Circulation* 2002;106:1368–73 CrossRef Medline
29. Iwata T, Mori T, Tajiri H, et al. **Successful stenting by combination technique of reverse flow and downstream filtering for long chronic total occlusion of the cervical vertebral artery: technical case report.** *Neurosurgery* 2009;65:E378–79 CrossRef Medline
30. Zhou Z, Li R, Zhao X, et al. **Evaluation of 3D multi-contrast joint intra-and extracranial vessel wall cardiovascular magnetic resonance.** *J Cardiovasc Magn Reson* 2015;17:41 CrossRef Medline
31. Liebeskind DS. **Collateral circulation.** *Stroke* 2003;34:2279–84 CrossRef Medline
32. Maas MB, Lev MH, Ay H, et al. **Collateral vessels on CT angiography predict outcome in acute ischemic stroke.** *Stroke* 2009;40:3001–05 CrossRef Medline
33. Truong M, Håkansson C, HaileMichael M, et al. **The potential role of T2*-weighted multi-echo data image combination as an imaging marker for intraplaque hemorrhage in carotid plaque imaging.** *BMC Med Imaging* 2021;21:121 CrossRef Medline
34. Saam T, Ferguson MS, Yarnykh VL, et al. **Quantitative evaluation of carotid plaque composition by in vivo MRI.** *Arterioscler Thromb Vasc Biol* 2005;25:234–39 CrossRef Medline
35. Sui B, Gao P. **High-resolution vessel wall magnetic resonance imaging of carotid and intracranial vessels.** *Acta Radiol* 2019;60:1329–40 CrossRef Medline
36. Joseph P, Ishai A, Mani V, et al. **Short-term changes in arterial inflammation predict long-term changes in atherosclerosis progression.** *Eur J Nucl Med Mol Imaging* 2017;44:141–50 CrossRef Medline
37. Paraskevas KI, Mikhailidis DP, Liapis CD. **Internal carotid artery occlusion: association with atherosclerotic disease in other arterial beds and vascular risk factors.** *Angiology* 2007;58:329–35 CrossRef Medline
38. Stone GW, Kandzari DE, Mehran R, et al. **Percutaneous recanalization of chronically occluded coronary arteries: a consensus document: Part I.** *Circulation* 2005;112:2364–72 CrossRef Medline
39. Tartari S, Rizzati R, Righi R, et al. **High-resolution MRI of carotid plaque with a neurovascular coil and contrast-enhanced MR angiography: one-stop shopping for the comprehensive assessment of carotid atherosclerosis.** *AJR Am J Roentgenol* 2011;196:1164–71 CrossRef Medline
40. Naghavi M, Libby P, Falk E, et al. **From vulnerable plaque to vulnerable patient: a call for new definitions and risk assessment strategies: Part I.** *Circulation* 2003;108:1664–72 CrossRef Medline
41. Archie JP Jr. **Carotid endarterectomy when the distal internal carotid artery is small or poorly visualized.** *J Vasc Surg* 1994;19:23–30 CrossRef Medline
42. Morais LT, Leslie-Mazwi TM, Lev MH, et al. **Imaging-based selection for intra-arterial stroke therapies.** *J Neurointerv Surg* 2013;5 (Suppl 1):i13–20 CrossRef Medline
43. Furie B, Furie BC. **Mechanisms of thrombus formation.** *N Engl J Med* 2008;359:938–49 CrossRef Medline
44. Marder VJ, Chute DJ, Starkman S, et al. **Analysis of thrombi retrieved from cerebral arteries of patients with acute ischemic stroke.** *Stroke* 2006;37:2086–93 CrossRef Medline
45. Saha P, Andia ME, Modarai B, et al. **Magnetic resonance T-1 relaxation time of venous thrombus is determined by iron processing and predicts susceptibility to lysis.** *Circulation* 2013;128:729–36 CrossRef Medline
46. U-King-Im JM, Fox AJ, Aviv RI, et al. **Characterization of carotid plaque hemorrhage: a CT angiography and MR intraplaque hemorrhage study.** *Stroke* 2010;41:1623–29 CrossRef Medline
47. Trelles M, Eberhardt KM, Buchholz M, et al. **CTA for screening of complicated atherosclerotic carotid plaque: American Heart Association type VI lesions as defined by MRI.** *AJNR Am J Neuroradiol* 2013;34:2331–37 CrossRef Medline
48. Bitar R, Moody AR, Leung G, et al. **In vivo 3D high-spatial-resolution MR imaging of intraplaque hemorrhage.** *Radiology* 2008;249:259–67 CrossRef Medline
49. Saba L, Yuan C, Hatsukami TS, et al; Vessel Wall Imaging Study Group of the American Society of Neuroradiology. **Carotid artery wall imaging: perspective and guidelines from the ASNR Vessel Wall Imaging Study Group and Expert Consensus Recommendations of the American Society of Neuroradiology.** *AJNR Am J Neuroradiol* 2018;39:E9–31 CrossRef Medline